(BL2B1)

Adsorbed states of chemisorbed and physisorbed N2 on Pd(110)

Jun Yoshinobu[1,2], Hiroyuki Kato[1], Hiroshi Okuyama[1], Hirohito Ogasawara[1], Tadahiro Komeda[1], Maki Kawai[1], Shin-ichiro Tanaka[3] and Masao Kamada[3]

1) The Institute of Physical and Chemical Research (RIKEN), 2-1 Hirosawa, Wako 351-0198. 2) The Institute for Solid State Physics, The University of Tokyo, 7-22-1 Roppongi, Minato-ku, Tokyo 106-6666. 3) Institute for Molecular Science, Myodaiji-cho, Okazaki 444-8585 .

Adsorption states of N_2 on Pd(110) at low temperature (20-100K) have been studied by means of high resolution electron energy loss spectroscopy (HREELS), photoelectron spectroscopy (PES), thermal desorption spectroscopy (TDS), low energy electron diffraction (LEED) and near edge X-ray absorption fine structure (NEXAFS)

At ~0.1 ML (monolayer) at 20K, two losses at 30 and 280 meV are observed in the specular direction in addition to the Pd(110) surface resonance peak at 18 meV [1]. According to the previous study [2], these peaks were attributed to Pd-N_2 stretching mode and N_2 stretching mode, respectively. By the off-specular mode, a hindered rotational mode is newly observed at ~25 meV. A p(2x1) LEED is observed at 0.5 ML [2]. The structure is a upright linear configuration according to the NEXAFS experiments.

With increasing the coverage, a peak assigned to the hindered rotational mode becomes visible at ~25 meV in the specular direction. At the saturation with adsorbed N_2 on Pd(110) at 50 K, loss peaks are observed at 24, 29 and 278 meV. Thus, the orientation of the molecule is tilted above 0.5 ML due to the intermolecular interaction.

From the TDS results, the desorption peaks are observed at ~85 K and 105 K. These N_2 species are chemisorbed on Pd(110) since the hybridization occurs between N_2 orbitals (mainly 1π, 5σ and 2π) and Pd valence band according to the PES results.

With increasing the coverage at 30 K, the desorption peaks from physisorbed and multilayer N_2 are observed at ~50 K and 35 K, respectively. The PES results shows less perturbed N_2 orbitals where the binding energy difference between $3\sigma_g$, $1\pi_u$ and $2\sigma_u$ is similar to that of gaseous N_2 .

REFERENCE

[1] J. Yoshinobu et al., Phys. Rev. B **38**, 1520 (1988).

[2] Y. Kuwahara et al., Surf. Sci. **180**, 421 (1987).

(BL-2B1)

Effective Escape Depth of Photoelectrons for Hydrocarbon Films in Total Electron Yield Measurement at C *K*-edge

Hideaki Ohara[1], Yasushi Yamamoto[1], Kotaro Kajikawa[1], Hisao Ishii[1], Kazuhiko Seki[1,2] and Yukio Ouchi[1]

[1]*Department of Chemistry, Graduate School of Science, Nagoya University, Chikusa-ku, Nagoya 464-8602, Japan*
[2]*Research Center for Materials Science, Nagoya University, Nagoya 464-8602, Japan*

When investigating molecular conformations and orientations in organic thin films by Near Edge X-ray Absorption Fine Structure (NEXAFS), we often need to pay attention to the escape depth L of materials, which depends on an electron-detection method. In the case of Auger electron yield mode, the escape depth of the Auger electron can be easily estimated since an electron energy dependence of the escape depth has been measured[1][2][3]. On the other hand, in total electron yield (TEY) mode of detection, which is also commonly used, photoelectrons suffer multiple scattering and exact escape depth is difficult to obtain due to the lack of information for secondary photoelectrons. Reliable information on L_{eff} for C *K*-edge TEY mode is still lacking.

In this study, we performed NEXAFS and AFM measurements for multilayer systems to deduce the L_{eff} at C *K*-edge TEY mode. The sample used in our experiment was a HTC (hexatriacontane, n-$C_{36}H_{74}$) /polyimide (biphenyl-3,3',4,4'-tetracarboxylic dianhydride type) / Si multilayer. Quantitative degrees of superposition of C *K*-edge spectra of HTC and polyimide with aromatic rings were evaluated to obtain L_{eff}.

The multilayer-sample were prepared as follows : To begin with, polyimide / NMP (N-methyl-2-pyrolidone) solution was spin-coated on a Si substrate. Then, HTC was evaporated on the polyimide. Three samples with different HTC thicknesses (#0 : 0 Å, #1 : 70 Å and #2 : 94 Å) monitored by a quartz oscillator were prepared. C *K*-edge NEXAFS spectra were taken at BL-2B1. Measurements were performed in TEY mode with normal incidence under a vacuum of 10^{-8} Pa range. AFM images of the sample were taken in dynamic force mode (DFM) not to damage the HTC layers. Ten AFM images ($10\mu m \times 10\mu m$) at different positions of each sample were taken and then averaged.

In Fig.1, we summarize C *K*-edge NEXAFS spectra for various HTC thicknesses. Peak (a) has already been assigned as C1s$\rightarrow \pi^*$(C=C) resonance[4][5], so this peak is originated from the polyimide layer. Figure 2 shows a typical example of AFM images of sample #1. Evaporated HTC molecules onto polyimide formed islands (or domains) with different thickness and the height of one step was nearly equal to 47 Å corresponding to a full length of HTC molecule. The values of L_{eff} were determined with use of a following formula ;

$$I / I_0 = \sum_{i=0} S_i \exp\left(-d \cdot i / L_{eff}\right)$$

where d is the thickness of one HTC layer (47 Å) and i is the number of the layers in the domain, respectively. S_i refers to the ratio of the domain size of corresponding thicknesses. Peak (a) intensity of samples #1 and #2 normalized by that of #0 (no HTC evaporated) gives I / I_0. Values obtained are listed in Table.1. As is shown in Table.1, L_{eff} range from 30 Å to 39 Å. An experimental error of L_{eff} ; mainly due to the inaccuracy in the evaluation of the domain size. These values are still quite reasonable when we consider NEXAFS studies on the surface freezing effect of pentacontane (PC, n-$C_{50}H_{102}$)[6], where a inclined PC monolayer is formed on top of the PC liquid phase for a couple of degrees. The tilt angle of PC deduced from TEY measurement is greater than those determined by X-ray diffraction. However, when account is taken of L_{eff}, the agreement between the X-ray diffraction and TEY measurements improve considerably demonstrating the importance of determining escape length of photoelectrons which are used in detection method.

References

[1]Cartier, E., Pfluger, P., Pireaux. and Rei Vilar, M. (1987). Appl. Phys. A44, 43-53.
[2]Bain, C. D., Whitesides, G. M. (1989). J. Phys. Chem. 93, 1670-1673.
[3]Laibinis, P. E., Bain, C. D. and Whitesides, G. M. (1991). J. Phys. Chem. 95, 7017-7021.

[4]Schedel, Th. - Niedrig et al. (1991). Ber. Bunsenges. Phys. Chem. 95, 1385.
[5]Jordan, J. L. - Sweet et al. (1988). J. Chem. Phys. 89, 2482.
[6]Yamamoto, Y., Mitsumoto, R., Ito, E., Araki, T., Ouchi, Y., Seki, K. and Takanishi, Y. (1996). J. Electron Spectrasc. 78, 367-370.

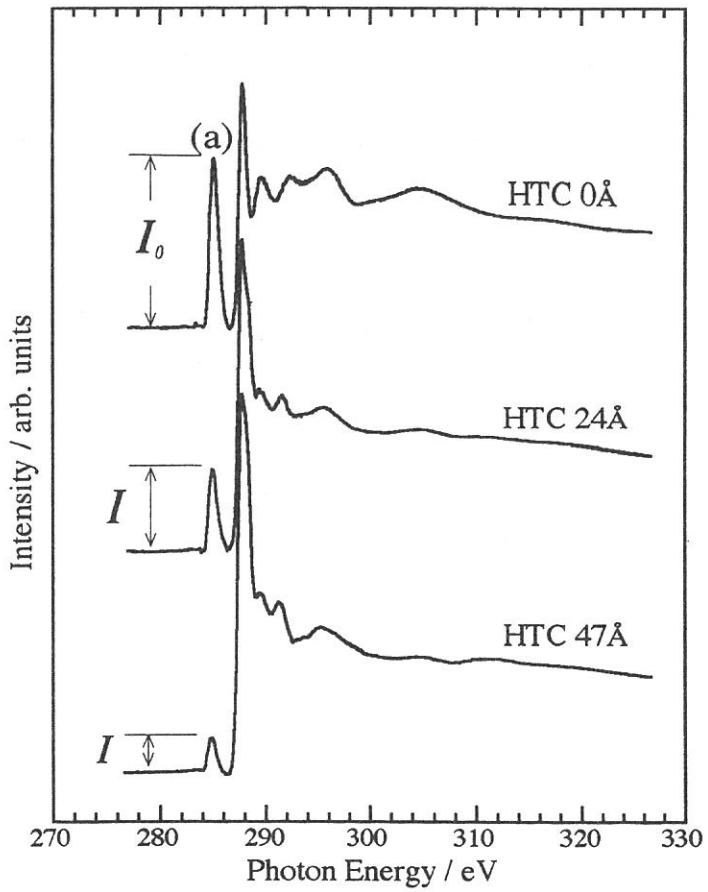

Fig.1. C K-edge NEXAFS spectra for various HTC thicknesses. Thicknesses are monitored by quartz oscillator.

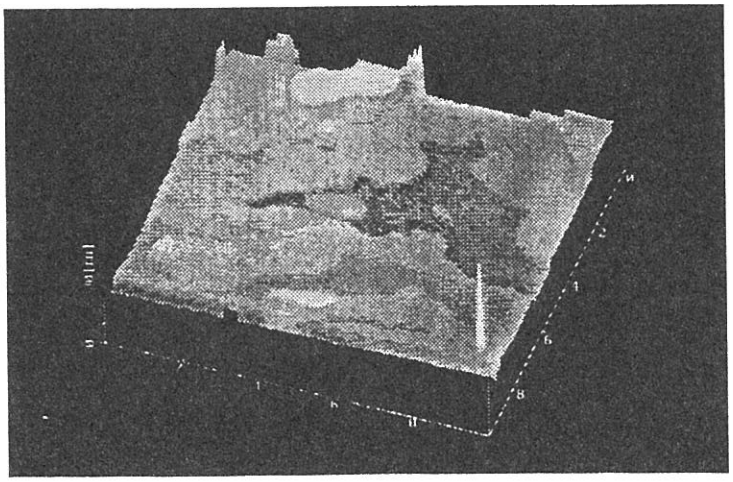

Fig.2 A typical example of AFM images of sample #1.

Table 1. Obtained effective escape depths.

Sample	I / I_0	L_{eff} / Å
#1	0.107	**39**
#2	0.065	**30**

(BL2B1)

Study of ion desorption induced by resonant core-electron excitations of condensed water using Auger electron-photoion coincidence spectroscopy

Kazuhiko Mase, Shin-ichiro Tanaka, Tsuneo Urisu, Eiji Ikenaga[1], and Kenichiro Tanaka[1]

Institute for Molecular Science, Okazaki 444-8585, Japan
[1]Faculty of Science, Hiroshima University, Higashi Hiroshima 739, Japan

Ion desorption mechanism in the region of resonant excitations of Oxygen 1*s* core-electron of condensed water is studied using Auger electron-photoion coincidence (AEPICO) spectroscopy. A newly developed coincidence analyzer was used for which the resolution of the electron kinetic energy was improved to E/△ E = 100. Figure 1 shows Auger electron yield (AEY, electron kinetic energy: 490 eV), total ion yield (TIY) and TIY/AEY spectra of condensed H_2O in the oxygen K-edge region. The TIY/AEY spectrum exhibited a characteristic threshold peak at the $4a_1 \leftarrow$ O:1*s* resonance ($h\nu$ = 532.3 eV) and a suppression at the $3p \leftarrow$ O:1*s* resonance ($h\nu$ = 535.5 eV). Figure 2 shows the electron kinetic energy dependence of the AEPICO yield (AEPICO yield spectra) at $h\nu$ = 532.6, 533.6, 335.4, 540.6, 547.6, and 557.8 eV. At the $4a_1 \leftarrow$ O:1*s* resonance ($h\nu$ = 532.6 eV) and $2b_2 \leftarrow$ O:1*s* resonance ($h\nu$ = 533.6 eV), the AEPICO yield spectrum exhibited major, medium and minor peaks at the electron kinetic energies of 502.5, 482.5, and 465 eV, which are assigned to $(O{:}2p)^{-2}(4a_1(\text{or } 2b_2))^1$, $(O{:}2s)^{-1}(O{:}2p)^{-1}(4a_1(\text{or } 2b_2))^1$, and $(O{:}2s)^{-2}(4a_1(\text{or } 2b_2))^1$ spectator Auger final states, respectively. These results shows that ultrafast ion desorption mechanism is predominant at the $4a_1$ and $2b_2$ resonances. The enhancement of the H^+ AEPICO yield was attributed to the strongly O-H antibonding character of the $4a_1$ and $2b_2$ orbitals. At the 3*p* resonance ($h\nu$ = 535.4 eV), the AEPICO yield spectrum exhibited major, medium and minor peaks at the electron kinetic energies of 460, 475, and 490 eV, which are assigned to $(2a_1)^{-2}(3p)^1$, $(2a_1)^{-1}(1b_2)^{-1}(3p)^1$, and $(1b_2)^{-2}(3p)^1$ spectator Auger final states, respectively. This result indicates that spectator Auger stimulated ion desorption mechanism is responsible at the 3*p* resonance. The suppression of the H^+ AEPICO yield was attributed to the reduction of the hole-hole Coulomb repulsion due to the 3*p* electron. At $h\nu$ = 540.6, 547.6 and 557.8 eV, the AEPICO yield spectrum exhibited three peaks at the electron kinetic energies of 460, 475, and 490 eV, which are assigned to $(2a_1)^{-2}$, $(2a_1)^{-1}(1b_2)^{-1}$, and $(1b_2)^{-2}$ normal Auger final states, respectively. This result

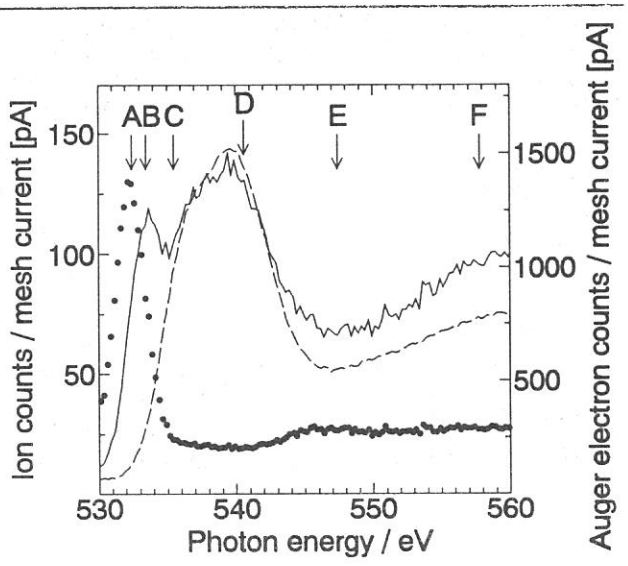

Figure 1. Total ion yield (TIY) spectrum (——), Auger electron yield (AEY) spectrum (----), and TIY/AEY spectrum of condensed H_2O (……).

indicates that the normal Auger stimulated ion desorption mechanism is responsible at photon energies above the O:1*s* ionization. These results and conclusions are consistent with the previous study carried out by low-resolution AEPICO spectroscopy [1].

Reference

[1] K. Mase, M. Nagasono, S. Tanaka, T. Urisu, E. Ikenaga, T. Sekitani, and K. Tanaka, *J. Chem. Phys.* **108**, 6550 (1998).

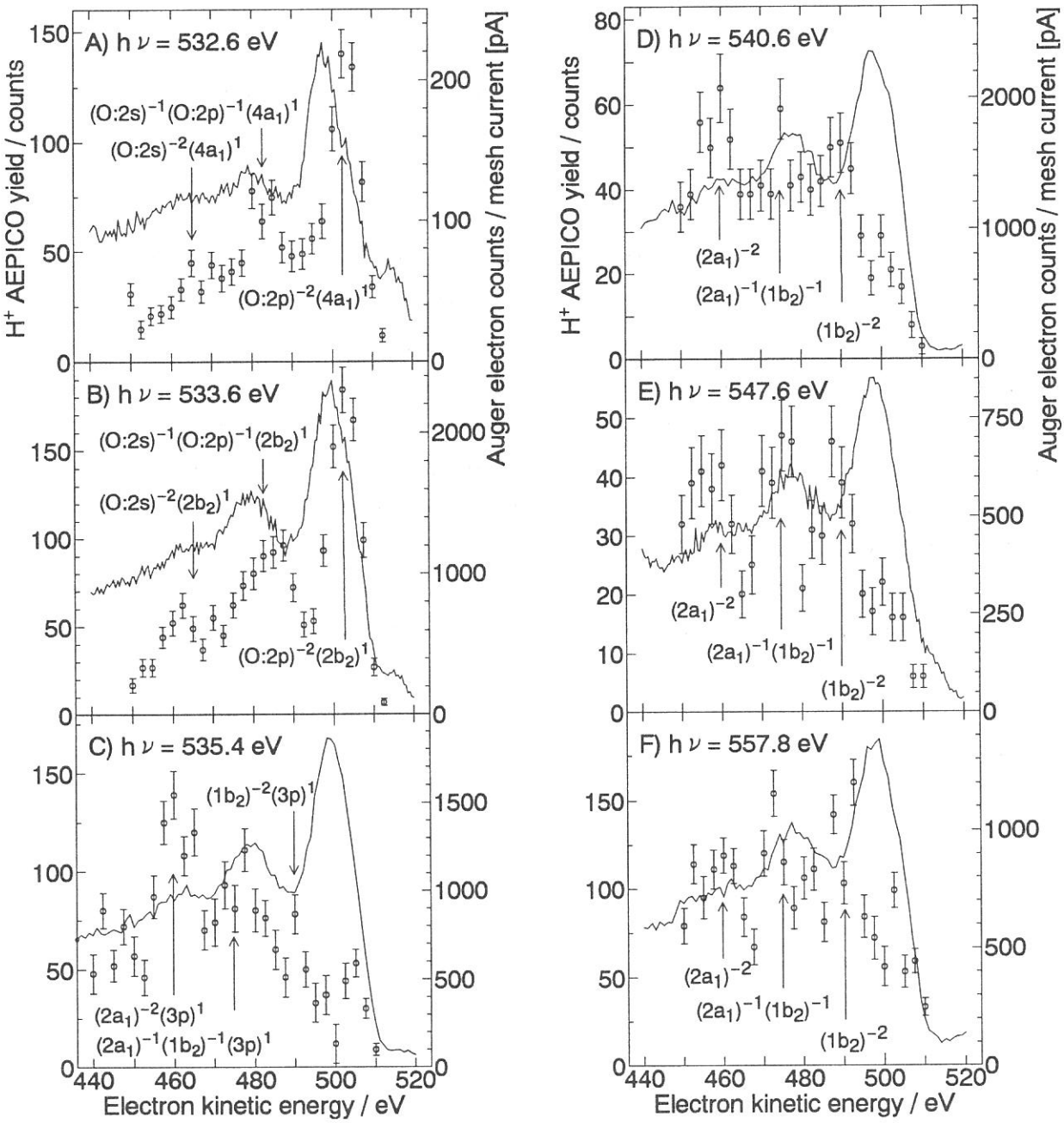

Figure 2. H^+ AEPICO yield spectra at $h\nu$ = A)532.6, B)533.6, C)535.4, D)540.6, E)547.6, and F)557.8 eV. The solid lines show typical Auger electron spectra.

(BL2B1)

Site-specific fragmentation following C:1*s* core-level photoionization of $CF_3CH(OH)CH_3$ adsorbed on a Si(100) surface

Arinobu Nakamura, Shin-ichi Nagaoka, Kazuhiko Mase,[A] Shin-ichiro Tanaka[A] and Tsuneo Urisu[A]

Department of Chemistry, Faculty of Science, Ehime University, Matsuyama 790-8577

[A]Institute for Molecular Science, Okazaki 444-8585

Synchrotron radiation has provided a powerful means to obtain information about core-level excitations, and the dynamic processes following the core-level excitations in molecules have long been a subject of interest. In contrast to valence electrons that are often delocalized over the entire molecule, the core electrons are localized near the atom of origin. Although core electrons do not participate in the chemical bonding, the energy of an atomic core-level in the molecule depends on the chemical environment around the atom. A shift in the energy levels of core electrons that is due to a specific chemical environment is called a chemical shift.

Monochromatized synchrotron radiation can excite core electrons of an atom in a specific chemical environment selectively, discriminating the core electrons from those of like atoms having different chemical environments. This site-specific excitation often results in site-specific fragmentation, which is of importance in understanding localization phenomena in chemical reactions and which is potentially useful for synthesizing materials through selective bond breaking. Synchrotron radiation can indeed play the part of an optical knife for molecules. When bond dissociation around an atomic site is required in the synthesis, one can use the optical knife that has the photon energy corresponding to the specific excitation of that site.

To elucidate the site-specific fragmentation, we have studied the spectroscopy and dynamics following core-level photoionization of various molecules condensed on surfaces [1,2]. To observe the dissociation processes following core-level ionization of a site selectively, we use the energy-selected-photoelectron photoion coincidence (ESPEPICO). The measurements of fragment ions coincidentally produced with energy-selected photoelectrons allow selective observation of the processes initiated by the electron ejection.

In the present work, we have used photoelectron spectroscopy and the ESPEPICO method to study the site-specific fragmentation following C:1*s* photoionization of $CF_3CH(OH)CH_3$ (TFIP) adsorbeded on a Si(100) surface. TFIP is expected to be adsorbed on Si(100) like $CF_3CH(OSi\{substrate\})CH_3$ [3]. The chemical environments of a C atom bonded to three F atoms (C[F]), of C bonded to three H atoms (C[H]) and of C bonded to H and OSi (C[OSi]) are different from one another, so it seems likely that TFIP will show site-specific fragmentation. In a monolayer regime, competition between surface reactions and electronic relaxation is expected to make the site-specific phenomena complex.

Figure 1 shows the photoelectron spectrum of TFIP in the region of C:1*s* electron emission. The low-resolution photoelectron spectrum shown in the main panel has two peaks in this region.

The peak at the higher-energy side is thought to correspond to C[F]:1*s* electron emission. The high-resolution spectrum of the peak at the lower-energy side is shown in the inset. The peak at the lower-energy side is found to be a doublet. The shoulders at the lower- and higher-energy sides in the inset are thought to correspond to C[OSi]:1*s* and C[H]:1*s* electron emissions, respectively.

Figures 2a, b and c show the ESPEPICO spectra obtained with emissions of the C[OSi]:1*s*, C[H]:1*s* and C[F]:1*s* electrons, respectively. These spectra were obtained with emissions of the C:1*s* electrons whose binding energy are indicated by arrows in Fig. 1. H^+ ion is predominantly desorbed coincidentally with the C[H]:1*s* and C[OSi]:1*s* electrons. In contrast, F^+ ion is predominantly desorbed coincidentally with the C[F]:1*s* electron. The ionic fragmentation occurs selectively around the C atom where the photoionization has taken place: synchrotron radiation can indeed play the part of an optical knife for molecules.

[1] S. Nagaoka, K. Mase, M. Nagasono, S. Tanaka, T. Urisu and J. Ohshita, J. Chem. Phys. 107, 10751 (1997).

[2] S. Nagaoka, K. Mase and I. Koyano, Trends Chem. Phys. 6, 1 (1997).

[3] J. Yoshinobu, S. Tanaka, and M. Nishijima, Appl. Phys. 60, 1196 (1991).

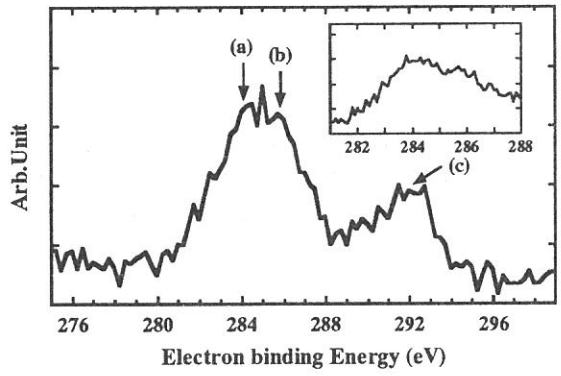

Figure 1

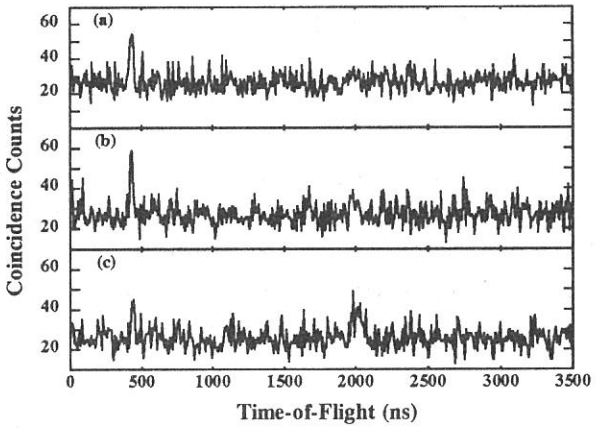

Figure 2

Figure 1 (left-hand side). Photoelectron spectrum of TFIP adsorbed on a Si(100) surface. The low-resolution photoelectron spectrum in the region of C:1*s* electron emission is shown in the main panel. The high-resolution spectrum of the peak at the lower-energy side is shown in the inset. The spectra in the main panel and the inset were taken at photon energies of 404.1 and 310.9 eV, respectively. Each of the channels in the main panel was measured for 2 s at a step 0.25 eV and each of those in the inset was measured for 8 s at 0.1 eV. An electronic field across the ionization region was applied during the measurement of the main panel.

Figure 2 (right-hand side). ESPEPICO spectra of TFIP adsorbed on a Si(100) surface. These spectra were obtained with emissions of the C:1s electrons whose binding energy are indicated by arrows in Fig. 1. The spectra were taken at a photon energy of 404.1 eV and the data collection time was 11700 s. (a) C[OSi]:1*s* electron emission. (b) C[H]:1*s* electron emission. (c) C[F]:1*s* electron emission.

(BL2B1)

ORIENTATION OF OXYGEN ADMOLECULES ON STEPPED PLATINUM(133) AND (335) SURFACES

Manami Sano*, Yoshiyuki Seimiya, Toshiro Yamanaka, Yuichi Ohno, Tatsuo Matsushima, Shin-ichiro Tanaka** and Masao Kamada**

*Catalysis Research Center and *Graduate School of Environmental Earth Science, Hokkaido University, Sapporo 060-0811, Japan,*

*** Institute for Molecular Science, Myodaiji Okazaki 444-8585, Japan*

The orientation of oxygen ad-molecules was studied on stepped Pt(133)=(s)[3(111)x(111)] and Pt(335) =(s)4(111)x(001) surfaces by using thermal desorption spectroscopy (TDS) and near edge X-ray absorption fine structure (NEXAFS). Three ad-molecule desorption peaks were commonly found at around 230 K(α_1-O_2), and below 200 K (α_2-O_2 and α_3-O_2). The ad-molecules yielding α_1-O_2 on Pt(133) lie along surface troughs, and those yielding α_2-O_2 and α_3-O_2 lie on declining three-atom-wide terraces of a (111) structure and are largely rotated from the surface trough direction. On the other hand, four-atom-wide terraces on Pt(335) seem too wide to yield definitely-oriented molecules except for a small coverage range.

Experiments;

TDS was carried out in a conventional UHV chamber. NEXAFS experiments were conducted in a chamber equipped with a Beam Line 2B1 using a grasshopper monochromator. The spectra were recorded by an Auger electron yield mode with the kinetic energy of the oxygen KLL Auger electrons at 520 eV. The angle of X-ray incidence (θ) was varied by rotating the sample crystal.

Results;

Pt(133); α_1-O_2 was oriented along the trough because the σ^* resonance was maximized and no π^* resonance appeared at the normal incidence of X-ray with the electric vector ($\vec{E}$) oriented in the [$\bar{1}$10] direction, and no σ^* was confirmed for $\vec{E}$ in a plane perpendicular to it. The cross section ratio ($A_{\sigma/\pi}$) of the σ^* resonance to the π^* was estimated to be 3 from the incidence angle dependence of α_1-O_2. This value was used to determine the rotation angles of the other species. α_2-O_2 rotated 40° from the trough and α_3-O_2 60°.

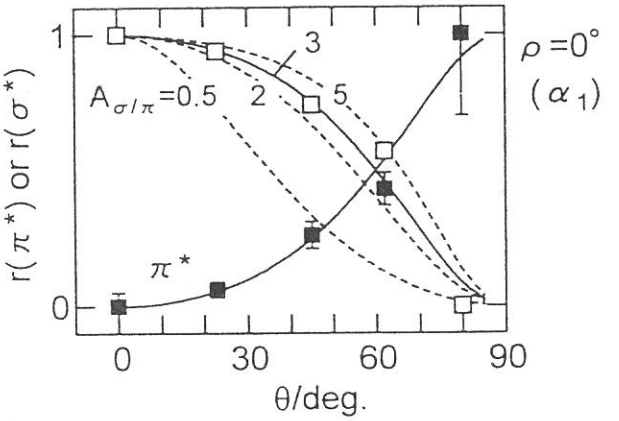

Fig. 1 NEXAFS cross section. The relative NEXAFS intensity ($A_{\sigma/\pi}$) of the π^* and σ^* resonance was determined from the incident angle dependence by assuming the definite orientation of α_1-O_2 along the trough on Pt(133). θ is the incidence angle of X-ray.

Pt(335); Oxygen ad-molecules were highly oriented along the trough at low coverages. NEXFAS spectrum showed that when the coverage (Θ_{O2}) was less than 0.17, the π^* resonance was much less than the σ^* at the normal incidence of X-ray with $\vec{E}$ in the [$\bar{1}$10] direction. The fraction of the π^* resonance was less than 10 % when $\vec{E}$ was oriented in the [$\bar{1}$10]

direction. The incidence angle dependence was plotted in Fig. 2b. The simulation with the ratio of $A_{\sigma/\pi}$=3 yielded the rotation angle of 20° from the trough direction. A comparison with the above results on Pt(133) suggests that α_1-O_2 limited at lower coverages is more oriented along the trough. This coverage may exceed the threshold value of α_1-O_2.

The additional oxygen molecules above this level showed enhanced π^* resonance and reduced σ^* signal as shown in Fig. 3. The contribution from these molecules was estimated as the difference between the signal at Θ_{O2}=0.17 and that at saturation. The π^* resonance shared about 20 % of the total yield. The incidence angle dependence is shown in Fig. 2c. This dependence would yield the rotation angle of 40° from the trough direction if these ad-molecules are assumed to be equally oriented only into two directional ways in the opposite manner (likely as $\pm\beta$°) from the trough direction. However, this orientation is not conclusive yet, because at least two forms of oxygen may be involved in these molecules. The surface modification method should be applied to prepare each oxygen ad-molecule separately.

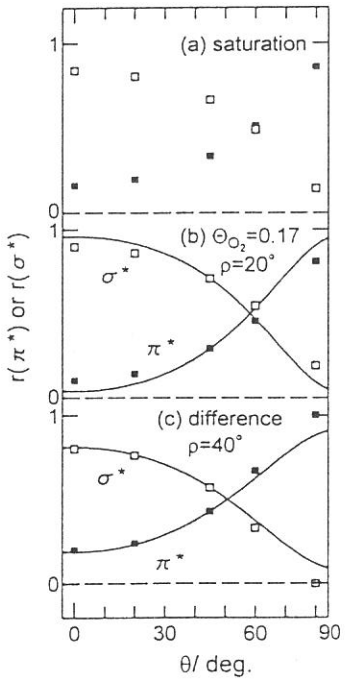

Fig. 2 NEXAFS intensity simulation.
The relative NEXAFS intensities of r(π^*) and r(σ^*) of oxygen at (a) saturation, (b) Θ_{O2}=0.17, and (c) coverage higher than this level are plotted as a function of the **E** orientation in a plane parallel to the step edge. The solid and open squares are from experimental results. The curves in (b) and (c) were calculated at $A_{\sigma/\pi}$ (cross-section ratio) = 3 and at ρ = 20 and 40°. ρ is the angle between the molecular axis and the trough direction. The declining terrace angle was assumed to be 14.5° .

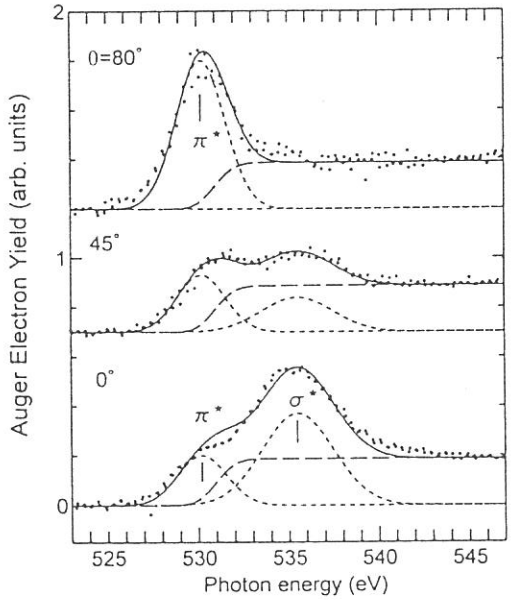

Fig. 3 NEXFAS of oxygen ad-molecules on Pt(335) at a high coverage and various incidence angles. The signal at Θ_{O2}=0.17 was subtracted from that at saturation.

1. Manami Sano, Yoshiyuki Seimiya, Yuichi Ohno, Tatsuo Matsushima, Shin-ichiro Tanaka, Masao Kamada, Appl. Surf. Sci. 130-132 (1998) 518.
2. Manami Sano, Yoshiyuki Seimiya, Yuichi Ohno, Tatsuo Matsushima, Shin-ichiro Tanaka, Masao Kamada, Surf. Sci. (1999) in press.

(BL2B1)

Ion desorption from TiO_2(110) surface

Shin-ichiro Tanaka, Kazuhiko Mase, Mitsuru Nagasono and Masao Kamada

Institute for Molecular Science, Okazaki, 444-8585, Japan

Desorption induced by the electronic transition (DIET) from the solid surfaces has been extensively studied for these decades, not only because it could be utilized as a tool for studying the atomic and electronic structures of solid surfaces, but also it is an important process of the photochemical reaction on the solid surface[1]. The mechanism of the ion desorption induced by the core-level excitation has been understood in a framework of the Knotek-Feibelman (KF) model[2]. Knotek and Feibelman observed the electron stimulated desorption (ESD) yield for the O^+ desorption from TiO_2 as a function of the incident electron energy, and found that the threshold of the desoprtion was corresponding to the threshold of the excitation from the Ti-3p level (not the O-2s level). In their model, the interatomic double Auger decay of the Ti-3p level results in the creation of the O^+ ion (it is O^{2-} in TiO_2), and the desorption occurs as a result of the repulsive force due to the Mardelung energy.

The electron –ion coincidence spectroscopy has been recently developed, and proved to be a very powerful tool for investigating the dynamics of the ion desorption induced by the core-level excitation and decay process[3]. In the present report, the ion desorption induced by the core-level excitation is investigated by using the synchrotron radiation and the electron-ion coincidence technique. All the experiments were carried out at the BL-2B1. The TiO_2(110) surface was cleaned by a number of cycles of Ar^+ ion sputtering and annealing. For avoiding the vacancy of oxygen at the surface, the sample was heated in the 10^{-6} Torr of oxygen jus before every measurement.

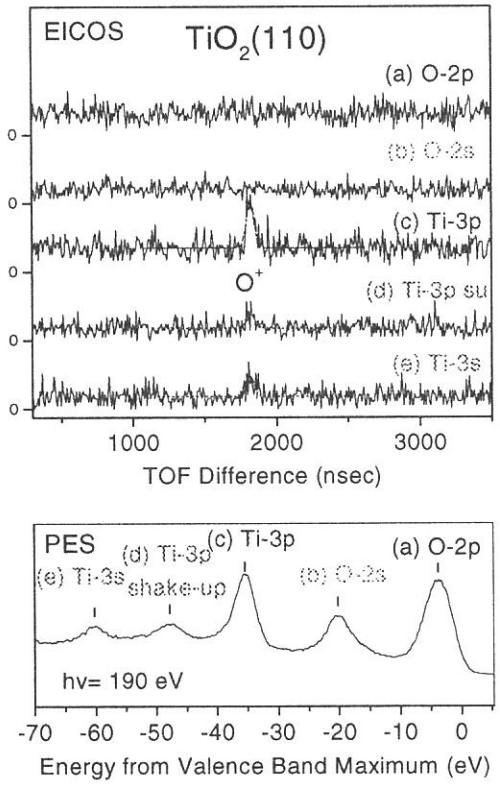

Figure 1 shows the coincidence spectra (upper part) and photoelectron spectrum (lower part) taken at hv=190 eV. The photoelectron spectrum shows the emission from the valence band (mainly O-2p) and from core levels of O-2s, Ti-3p and Ti-3s. A satellite peak due to the shake-up excitation of the Ti-3p level is also observed. The electron-ion coincidence spectra shows coincidence between ions and photoelectrons of the peaks indicated in the photoelectron spectrum. It is obvious that there are no peaks in the coincidence spectra of the valence (O-2p) and O-2s peaks [Fig. 1(a) and (b)] while O^+ peaks are observed for Ti-3p(c), Ti-3p shake-up (d) and Ti-3s(e) peaks. These results indicate that hole created via the photo-excitation of the valence and O-2s levels, meanwhile, the excitation of Ti-3p and Ti-3s levels yields the O^+ desorption. This is in agreement with the result of the electron stimulated desorption spectorscopy(ESDS) by Knotek et. al[2]. The desorption as a result of the direct process due to the excitation and decay can be distinguished from the desorption induced by the secondary electrons by using the coincidence technique, which was impossible in the ESDS technique. Father discussion will be made in a forthcoming paper.

[1] M. L. Knotek, Rep. Prog. Phys. **47**, 1499(1984); R.A. Rosenberg and V. Rehn, in *Synchrotron Radiation Research: Advances in surface and Interface Science, Vol. 2: Issues and Technology*, Ed. R.Z. Bachrach (Plenum Press, New York, 1992), p267.

[2] M.L. Knotek and P.J. Feibelman, Phys. Rev. Lett. **40**, 964(1978).; Surf Sci. **90**, 78(1979).

[3] K. Mase and M. Nagasono and S. Tanaka and M. Kamada and T.Urisu and Y. Murata, Rev. Sci. Inst., **68**, 1703(1997).